






## Article

# Heterologous Expression of Type II PKS Gene Cluster Leads to Diversified Angucyclines in *Streptomyces albus* J1074

Xiaoting Zhang <sup>1</sup>, Falei Zhang <sup>1</sup> , Chen Li <sup>1</sup>, Jiayi Li <sup>1</sup>, Xiao Xu <sup>1</sup>, Tianjiao Zhu <sup>1</sup> , Qian Che <sup>1</sup> , Deihai Li <sup>1,2,3</sup>   
and Guojian Zhang <sup>1,2,4,\*</sup> 

<sup>1</sup> Key Laboratory of Marine Drugs, Chinese Ministry of Education, School of Medicine and Pharmacy, Ocean University of China, Qingdao 266003, China

<sup>2</sup> Laboratory for Marine Drugs and Bioproducts, Qingdao Marine Science and Technology Center, Qingdao 266237, China

<sup>3</sup> Sanya Oceanographic Institute, Ocean University of China, Sanya 572025, China

<sup>4</sup> Marine Biomedical Research Institute of Qingdao, Qingdao 266101, China

\* Correspondence: zhangguojian@ouc.edu.cn

**Abstract:** Heterologous expression has emerged as an effective strategy in activating *Streptomyces* cryptic gene clusters or improving yield. Eight compounds were successfully obtained by heterologous expression of the type II PKS gene cluster *spi* derived from marine *Streptomyces* sp. HDN155000 in the chassis host *Streptomyces albus* J1074. The structures with absolute configurations were elucidated using extensive MS and NMR spectroscopic methods, as well as theoretical NMR calculations and electronic circular dichroism (ECD) calculations. Interestingly, compound WS009 Z (2) contains a rare thiomethyl group, angumycinone T (4) has a novel oxo-bridge formed between C12a and C4, and angumycinone X (3) showed cytotoxicity toward K562 and NCI-H446/EP cell lines.

**Keywords:** heterologous expression; II PKS; marine *Streptomyces*; angucycline



**Citation:** Zhang, X.; Zhang, F.; Li, C.; Li, J.; Xu, X.; Zhu, T.; Che, Q.; Li, D.; Zhang, G. Heterologous Expression of Type II PKS Gene Cluster Leads to Diversified Angucyclines in *Streptomyces albus* J1074. *Mar. Drugs* **2024**, *22*, 480. <https://doi.org/10.3390/md22110480>

Academic Editor: Cristina Sánchez-Porro

Received: 27 September 2024

Revised: 18 October 2024

Accepted: 18 October 2024

Published: 22 October 2024



**Copyright:** © 2024 by the authors. Licensee MDPI, Basel, Switzerland. This article is an open access article distributed under the terms and conditions of the Creative Commons Attribution (CC BY) license (<https://creativecommons.org/licenses/by/4.0/>).

## 1. Introduction

Angucyclines are a significant class of aromatic polyketide compounds biosynthesized by type II polyketide synthases (PKS) via an iterative Claisen condensation to generate Poly- $\beta$ -ketone backbones [1]. So far, over 400 members of angucyclines have been reported [2] and nearly half of them showed a wide range of biological activities, such as antimicrobial and/or anticancer, glutamate receptor agonist, gastric mucosal protectant, and platelet aggregation-inhibiting actions [3], which continually enhanced the importance of expanding the chemical space and obtaining novel angucycline derivatives for drug discovery and development purposes [4].

*Streptomyces*, a type of actinobacteria, is a Gram-positive bacterium with high GC genomes, primarily isolated from soil and marine sediments and other habitat samples [5–8], also known for its ability to produce a complex variety of secondary metabolites [9–11]. As genome sequencing technology advances, an increasing number of gene clusters (BGC) for natural products are being discovered [12]. However, only a limited number of natural products have been identified to date [13], making it essential to convert genomic information into valuable compounds for drug discovery and also commercial production. Heterologous expression of gene clusters is an effective strategy to address this problem by enabling the activation of cryptic gene clusters in heterologous host strains and increasing the yield of gene clusters expressed at low levels under laboratory conditions, as well as obtaining new analogues other than wild-type [14–16]. However, the biosynthetic capacity of an exogenous gene cluster is greatly affected by the metabolic characteristics of the chassis cells; for example, the competitive consuming of precursors in the native biosynthetic pathways will stop or drastically decrease the production of the desired compound. For this reason, it is critical to select a proper surrogate host, because different hosts influence the yield and

abundance of compounds, even possibly producing entirely distinct compounds [17,18]. Thus far, various *Streptomyces* species including *S. coelicolor*, *S. lividans*, *S. venezuelae*, *S. albus*, *S. fradiae*, *S. roseosporus*, and *S. toyocaensis* have been specifically engineered and frequently employed for heterologous expression [19].

During our ongoing research into bioactive chemicals from marine-derived microorganisms, six angucycline derivatives, including one novel oxaspirocyclic structure, were obtained by heterologous expression of a type II polyketide biosynthesis gene cluster *spi* in *Streptomyces coelicolor* A3(2) [20]. In the current study, to further explore the metabolic capacity of the BGC of *spi* and acquire more angucycline analogues, this cluster was expressed in another feasible heterologous host, *S. albus* J1074. A total of six angucycline derivatives and two by-products were obtained from the heterologous strains. Here, we will describe the construction of the recombinant strain, and the characterization of the structures obtained from the culture.

## 2. Results

### 2.1. Heterologous Expression of *spi* BGC in *S. albus* J1074

A type II PKS gene cluster *spi* (GenBank accession number OP009365, Figure 1a), which is responsible for angucyclines synthesis, has been previously identified and confirmed from the genome of a marine-derived actinobacteria strain of *Streptomyces* sp. HDN155000 [20]. To develop the metabolic potential of the *spi* BGC and obtain more angucycline analogues, we decided to have *spi* expressed in *S. albus* J1074, which has been demonstrated as a friendly surrogate host for heterologously expressing actinobacteria sourced genes due to its faster growth, small genome size, easy genetic manipulation procedure, and clear metabolic background [21–23]. The empty vector p15A was transferred into *S. albus* J1074 as the negative control (Figure 1b, trace i), and a series of new peaks were detected by HPLC analysis (Figure 1b, trace ii), demonstrating that the *spi* gene cluster was successfully activated and that changing heterologous host would greatly develop the metabolic capacity of the *spi* BGC (Figure S2).

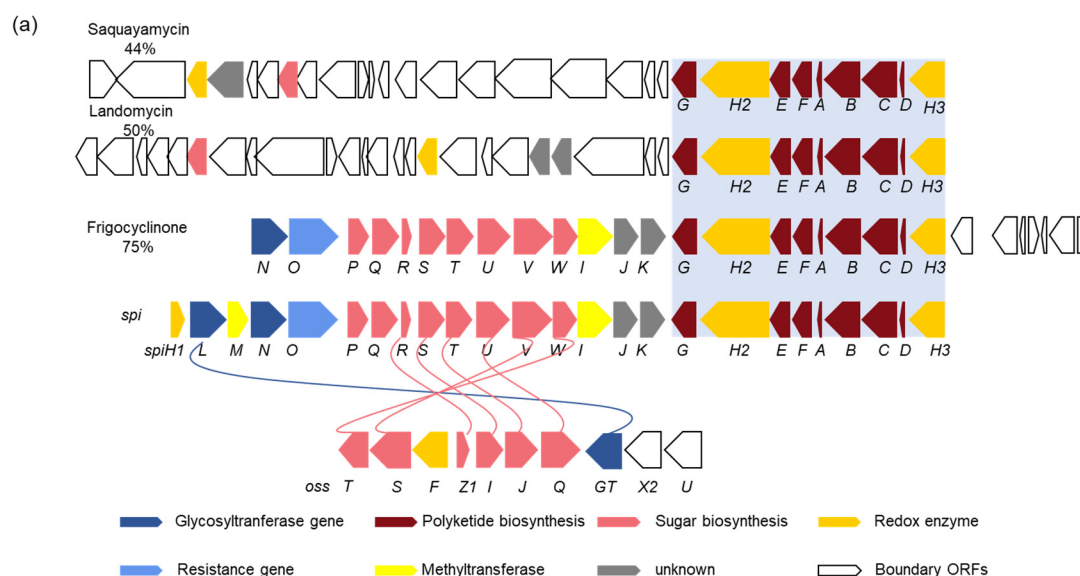
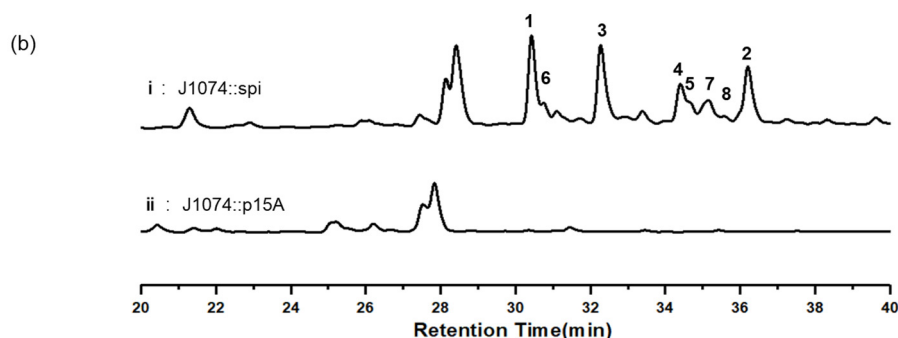


Figure 1. Cont.



**Figure 1.** (a) The *spi* gene cluster in comparison to homologous gene clusters that encode saquayamycin, landomycin, frigocyclinone, and ossamine (*oss*). (b) i: HPLC analysis of heterologous expression strain J1074::spi; ii: HPLC analysis of negative control host strain *S. albus* J1074::p15A.

## 2.2. Isolation and Purification of Compounds from Recombinant Strain

To specifically identify the compounds, we processed a larger-scale fermentation (20 L) of the strain J1074::spi, and ethyl acetate extraction of the fermentation product yielded 11.3 g crude extract. Subsequent stepwise separation by column chromatography (CC) with SiliaSphere C18 (ODS), medium pressure liquid chromatography (MPLC) and HPLC of the crude extract yielded a total of eight compounds, including four undescribed angucyclinone analogues: angumycinone Z (1) (7.1 mg), WS009 Z (2) (5.6 mg), angumycinone X (3) (6.4 mg), and angumycinone T (4) (4.7 mg). Compounds 5–8 were identified by comparing their 1D NMR and MS data to previously published literature (Figure 2).

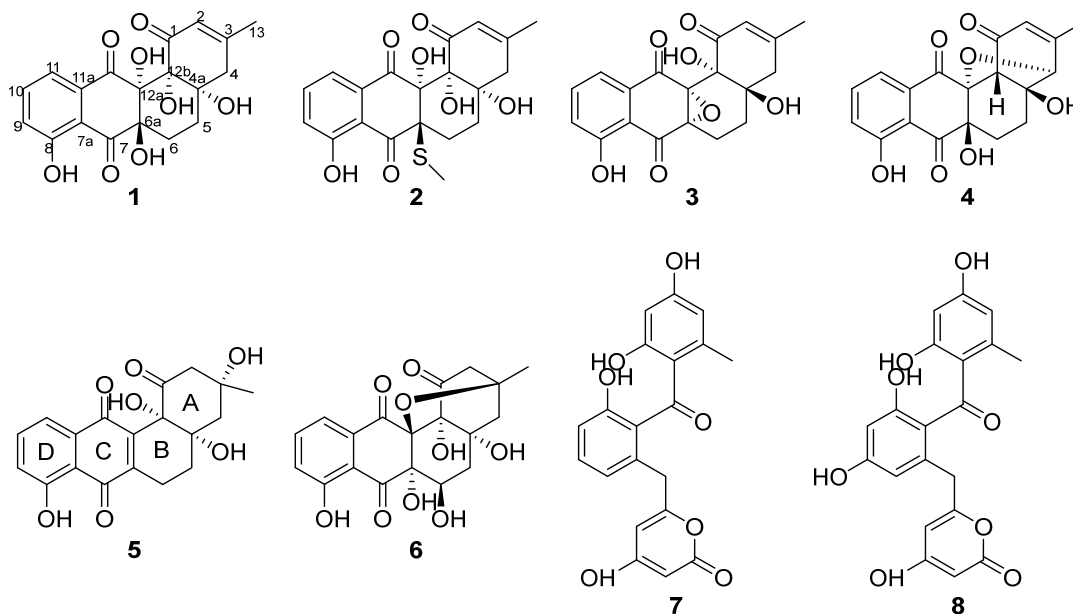


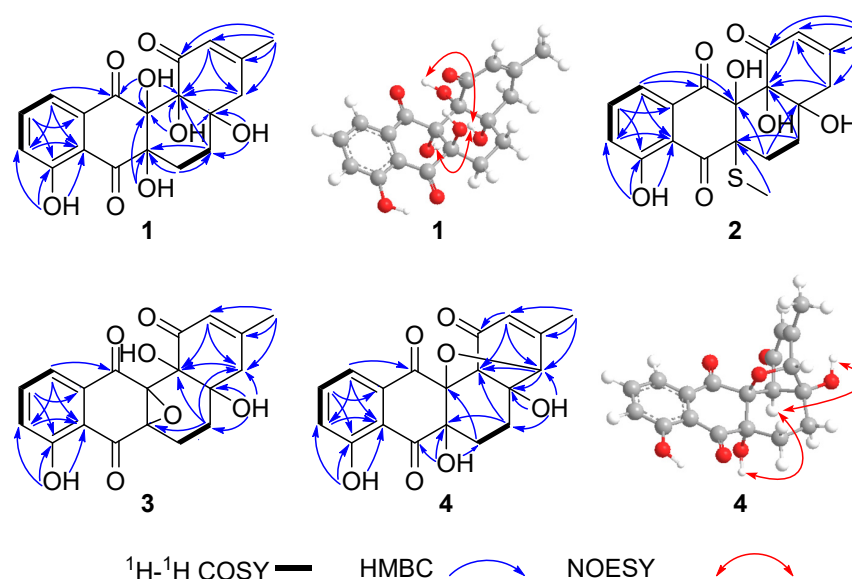
**Figure 2.** Chemical structures of 1–8.

Compound 1 was separated as a pale brown powder. Its molecular formula,  $C_{19}H_{18}O_8$ , was identified by HR-ESIMS  $m/z$  373.0916  $[M - H]^-$ , indicating eleven degrees of unsaturation. The signals indicated in the  $^1H$  NMR data illustrate that there are one methyl ( $\delta_H$  1.93, s), three methylenes ( $\delta_H$  2.89, 2.06;  $\delta_H$  1.98, 1.60;  $\delta_H$  2.28, 1.74), one vinyl methine ( $\delta_H$  5.71, s), three aromatic methines ( $\delta_H$  7.34, d,  $J = 8.2$  Hz;  $\delta_H$  7.76, t,  $J = 8.0$  Hz;  $\delta_H$  7.60, d,  $J = 7.5$  Hz), and five exchangeable protons ( $\delta_H$  11.10, s;  $\delta_H$  6.32, s;  $\delta_H$  6.03, s;  $\delta_H$  7.01, s;  $\delta_H$  5.66, s) (Table 1). The  $^{13}C$  NMR spectrum combined with the HSQC spectrum reveals the existence of one methyl, three  $sp^3$  methylenes, four protonated  $sp^2$  carbons, and eleven quaternary carbons (Table 2). These data imply that compound 1 has a tetracyclic benz[a]anthracene

skeleton belonging to the angucycline analogue [24,25], which possibly resulted from the expression of the *spi* BGC. The planar structure of **1** was subsequently identified through a comprehensive analysis of 2D NMR data (Figure 3). Firstly, the  $^1\text{H}$ - $^1\text{H}$  COSY correlations from H-9 ( $\delta_{\text{H}}$  7.34, d,  $J = 8.2$  Hz) via H-10 ( $\delta_{\text{H}}$  7.76, t,  $J = 8.0$  Hz) through H-11 ( $\delta_{\text{H}}$  7.60, d,  $J = 7.5$  Hz) indicate the presence of a 1,2,3-trisubstituted benzene ring (ring D) (Figure 3). The HMBC spectrum correlations from 8-OH ( $\delta_{\text{H}}$  11.10) to C-8 ( $\delta_{\text{C}}$  159.9, s), C-9 ( $\delta_{\text{C}}$  123.6, d), and C-7a ( $\delta_{\text{C}}$  116.3, s) showed a phenolic OH at C-8. The HMBC correlations from Me-13 to C-4 ( $\delta_{\text{C}}$  41.8, t), C-3 ( $\delta_{\text{C}}$  158.2, s), C-1 ( $\delta_{\text{C}}$  192.8, s), and C-2 ( $\delta_{\text{C}}$  122.9 d), from H-2 ( $\delta_{\text{H}}$  5.71, s) to C-4 and C-12b ( $\delta_{\text{C}}$  76.2, s), as well as from H-4 ( $\delta_{\text{H}}$  2.06, d,  $J = 17.7$  Hz) to C-4a ( $\delta_{\text{C}}$  75.5, s) and C-12b ( $\delta_{\text{C}}$  76.2, s) identified the presence of the A ring. The B ring was determined via the HMBC correlations from the active exchangeable protons 12a-OH ( $\delta_{\text{H}}$  7.01) to C-12a ( $\delta_{\text{C}}$  76.4, s), C-12 ( $\delta_{\text{C}}$  194.1, s), and C-12b ( $\delta_{\text{C}}$  76.2, s), from 12b-OH ( $\delta_{\text{H}}$  5.66) to C-4a ( $\delta_{\text{C}}$  75.5, s), C-12a ( $\delta_{\text{C}}$  76.4, s), and C-12b, from 4a-OH ( $\delta_{\text{H}}$  6.32) to C-4a, and C-5 ( $\delta_{\text{C}}$  28.2, t), and from 6a-OH ( $\delta_{\text{H}}$  6.03) to C-6a ( $\delta_{\text{C}}$  77.6, s) and C-12a ( $\delta_{\text{C}}$  76.4, s). The HMBC correlations from H-11 to C-12 and C-7 ( $\delta_{\text{C}}$  200.5, s) confirmed the connection of rings B and D via ring C. Thus, the planar structure of **1** was identified (Figure 3).

**Table 1.**  $^1\text{H}$  Spectroscopic Data for **1–4** in DMSO- $d_6$  (500 MHz).

No.	1	2	3	4
	$\delta_{\text{H}}$ (J in Hz)	$\delta_{\text{H}}$ (J in Hz)	$\delta_{\text{H}}$ (J in Hz)	$\delta_{\text{H}}$ (J in Hz)
2	5.71, s	5.70, s	5.97, s	5.83, s
4	2.89, d (18.0)	2.94, d (18.0)	3.06, d (18.0)	3.98, d (1.3)
	2.06, d (18.0)	2.13, d (18.0)	2.02, d (18.0)	-
5	1.98, m	2.07, m	1.76, m	1.98, m
	1.60, m	1.63, m	1.35, m	-
6	2.28, m	2.36, m	2.53, m	2.24, m
	1.74, m	1.84, m	2.38, m	2.14, m
9	7.34, d (8.0)	7.35, d (8.0)	7.31, m	7.35, dd (8.0, 1.0)
10	7.76, t (8.0)	7.73, t (8.0)	7.69, dd (8.2, 7.6)	7.76, dd (8.0, 7.6)
11	7.60, d (8.0)	7.58, d (8.0)	7.34, m	7.34, dd (7.6, 1.0)
12b	-	-	-	3.14, s
4a-OH	6.32, s	-	2.54, s	5.59, s
6a-OH	6.03, s	-	-	7.05, s
12a-OH	7.01, s	-	-	-
12b-OH	5.66, s	-	-	-
8-OH	11.10, s	11.17, s	11.06, s	11.72, s
13	1.93, s	1.96, s	1.81, s	2.33, d (1.2)
S-CH <sub>3</sub>	-	1.67, s	-	-

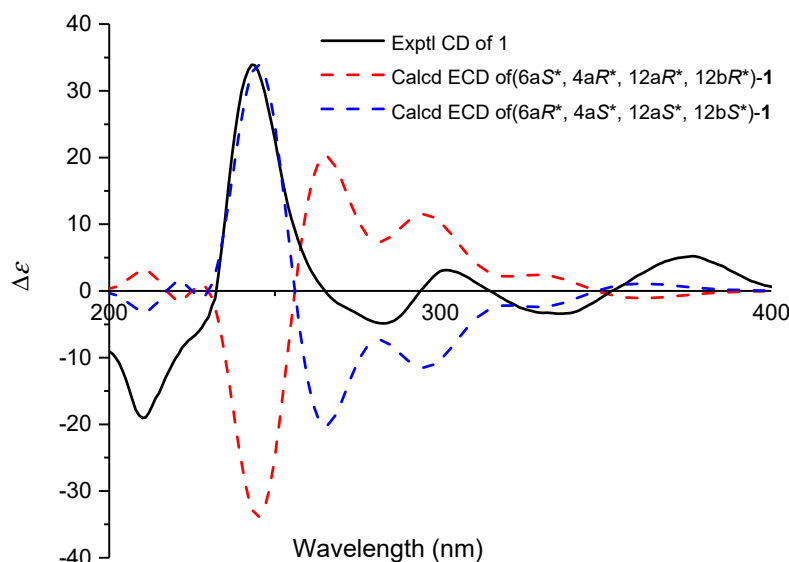


**Figure 3.**  $^1\text{H}$ - $^1\text{H}$  COSY, key HMBC and NOESY correlations of **1–4**.

**Table 2.**  $^{13}\text{C}$  Spectroscopic Data for 1–4 in DMSO- $d_6$  (125 MHz).

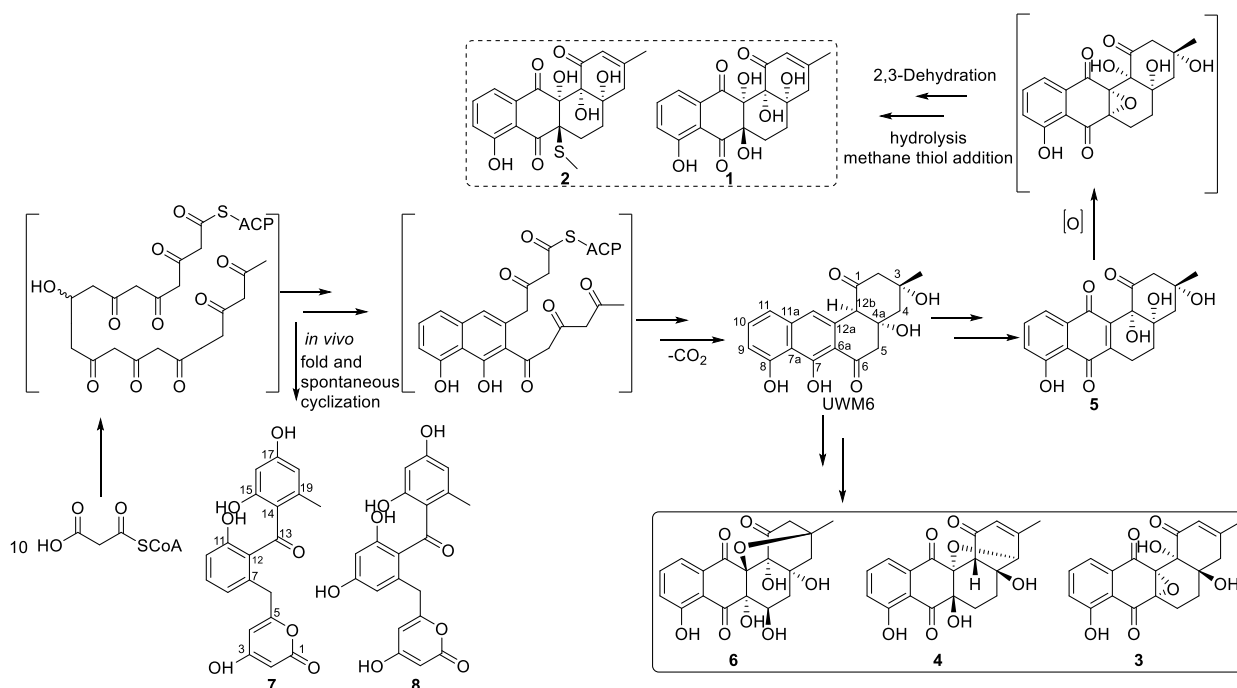
No.	1	2	3	4
	$\delta_{\text{C}}$ , Type	$\delta_{\text{C}}$ , Type	$\delta_{\text{C}}$ , Type	$\delta_{\text{C}}$ , Type
1	192.8, C	193.5, C	196.7, C	195.6, C
2	122.9, CH	122.7, CH	122.6, CH	124.6, CH
3	158.2, C	159.4, C	156.1, C	162.4, C
4	41.8, CH <sub>2</sub>	41.6, CH <sub>2</sub>	38.2, CH <sub>2</sub>	85.1, CH
4a	75.5, C	75.7, C	65.1, C	81.6, C
5	28.2, CH <sub>2</sub>	28.8, CH <sub>2</sub>	25.8, CH <sub>2</sub>	32.6, CH <sub>2</sub>
6	21.6, CH <sub>2</sub>	17.9, CH <sub>2</sub>	20.1, CH <sub>2</sub>	26.8, CH <sub>2</sub>
6a	77.6, C	61.2, C	74.2, C	78.0, C
7	200.5, C	195.5, C	194.5, C	201.6, C
7a	116.3, C	115.4, C	114.7, C	114.9, C
8	159.9, C	160.0, C	159.5, C	161.1, C
9	123.6, CH	124.4, CH	123.9, CH	123.7, CH
10	136.2, CH	136.0, CH	136.4, CH	137.7, CH
11	118.9, CH	119.0, CH	118.9, CH	118.3, CH
11a	133.0, C	131.5, C	132.7, C	135.3, C
12	194.1, C	191.0, C	189.6, C	192.1, C
12a	76.4, C	78.4, C	67.5, C	92.5, C
12b	76.2, C	75.7, C	73.7, C	52.7, CH
13	23.6, CH <sub>3</sub>	23.7, CH <sub>3</sub>	23.6, CH <sub>3</sub>	26.3, CH <sub>3</sub>
S-CH <sub>3</sub>	-	13.3, CH <sub>3</sub>	-	-

The absolute configuration of **1** was determined by NOESY spectrum analysis and ECD calculations. Analyzing the NOESY spectrum data revealed a correlation between 4a-OH ( $\delta_{\text{H}}$  6.32) and 12a-OH ( $\delta_{\text{H}}$  7.01), as well as a correlation between 4a-OH and 12b-OH ( $\delta_{\text{H}}$  5.66), while there was no correlation with 6a-OH ( $\delta_{\text{H}}$  6.03), which indicated that 4a-OH, 12a-OH, and 12b-OH were all in the same plane and 6a-OH was on the opposite side. Thus, the relative configuration of **1** was confirmed to be (6a*S*\*, 4a*R*\*, 12a*R*\*, 12b*R*\*)-**1** or (6a*R*\*, 4a*S*\*, 12a*S*\*, 12b*S*\*)-**1**. ECD calculation demonstrated that the latter was more compatible with the measured values, based on which the absolute configuration of compound **1** was confirmed as (6a*R*, 4a*S*, 12a*S*, 12b*S*)-**1** (Figure 4).

**Figure 4.** Calculated and experimental ECD spectra of **1**.

Compound **2** is an even brown amorphous powder with a molecular formula of  $\text{C}_{20}\text{H}_{20}\text{O}_7\text{S}$  given based on HRESIMS data. One-dimensional NMR and HSQC spectra showed that there were two methyl ( $\delta_{\text{C}}$  23.7 and 13.3), three  $\text{sp}^3$  methylenes ( $\delta_{\text{C}}$  17.9, 28.8, and 41.6), four protonated  $\text{sp}^2$  carbons ( $\delta_{\text{C}}$  119.0, 122.7, 124.4, and 136.0), and eleven quaternary carbons including four non-protonated  $\text{sp}^3$  carbons ( $\delta_{\text{C}}$  61.2, 75.7, 75.7, and 78.4),

four non-protonated sp<sup>2</sup> carbons ( $\delta_C$  115.4, 131.5, 159.4, and 160.0), and three carbonyls ( $\delta_C$  191.0, 193.5, and 195.5) (Table 2). These signals all indicate that compound **2** has a backbone highly similar to **1**. The difference lies in the high-field chemical shift of C-6 ( $\delta_C$  17.9, t), C-6a ( $\delta_C$  61.2, s), and C-7 ( $\delta_C$  195.5, s), recombined with the HMBC correlation from -SCH<sub>3</sub> ( $\delta_H$  1.67) to C-6a (Figure 3) and the HR-ESIMS data, which determined that the hydroxyl signal (6a-OH) in compound **1** was replaced by the thiomethyl group ( $\delta_C$  13.3, q) in **2**. However, the NOESY data could not determine the relative configuration of the thiomethyl group and three hydroxyl groups. Compounds **2** and **1** are proposed to have originated from the same epoxide precursor (discussed later in Scheme 1), which went through a ring opening process probably promoted by hydrolysis or methane thiol addition, hence the absolute configuration of **2** was tentatively assigned as 6a*R*, 4a*S*, 12a*S*, 12b*S*.



**Scheme 1.** Proposed biosynthetic pathways of compounds **1**–**8**.

Compound **3** is a yellowish solid powder. HR-ESIMS analysis established the chemical formula as C<sub>19</sub>H<sub>16</sub>O<sub>7</sub>, with twelve degrees of unsaturation. The <sup>1</sup>H and <sup>13</sup>C NMR spectra revealed that **3** contains one methyl, three methylene, four methenyl, and 11 quaternary carbon signals (including three carbonyl and six aromatic quaternary carbons). The <sup>1</sup>H and <sup>13</sup>C NMR spectra showed that **3** was highly similar to angumycinone A [26], with the only difference being the low-field chemical shift at C-12a ( $\delta_C$  67.5), from which it can be deduced that there is hydroxylation at this position, thus determining the planar structure of compound **3**. Nevertheless, the relative configuration was unable to be defined by the NOESY data. The stereo-structure was determined based on NMR calculations, DP4+ analysis, and ECD calculations, primarily NMR calculations and DP4+ probability analyses of the four possible configurations (6a*S*<sup>\*</sup>, 12a*R*<sup>\*</sup>, 12b*S*<sup>\*</sup>, 4a*R*<sup>\*</sup>)-**3a**, (6a*S*<sup>\*</sup>, 12a*R*<sup>\*</sup>, 12b*R*<sup>\*</sup>, 4a*S*<sup>\*</sup>)-**3b**, (6a*S*<sup>\*</sup>, 12a*R*<sup>\*</sup>, 12b*S*<sup>\*</sup>, 4a*S*<sup>\*</sup>)-**3c**, and (6a*S*<sup>\*</sup>, 12a*R*<sup>\*</sup>, 12b*R*<sup>\*</sup>, 4a*R*<sup>\*</sup>)-**3d** at the B3LYP/6-311+G(d,p) level using PCM model in DMSO. The calculated results for **3d** ( $R^2 = 0.9958$ ) were more consistent with the experimental data than others (Figure S3). Furthermore, the DP4+ probability calculations identified **3d** with a 99.90% probability (Table S7). The absolute configuration of **3** was then determined to be 6a*S*,12a*R*,12b*R*,4a*R* through ECD calculation at the B3LYP/6-31+G(d,p)/B3LYP/6-31G(d) level was compared with the experimental ECD curve (Figure 5).

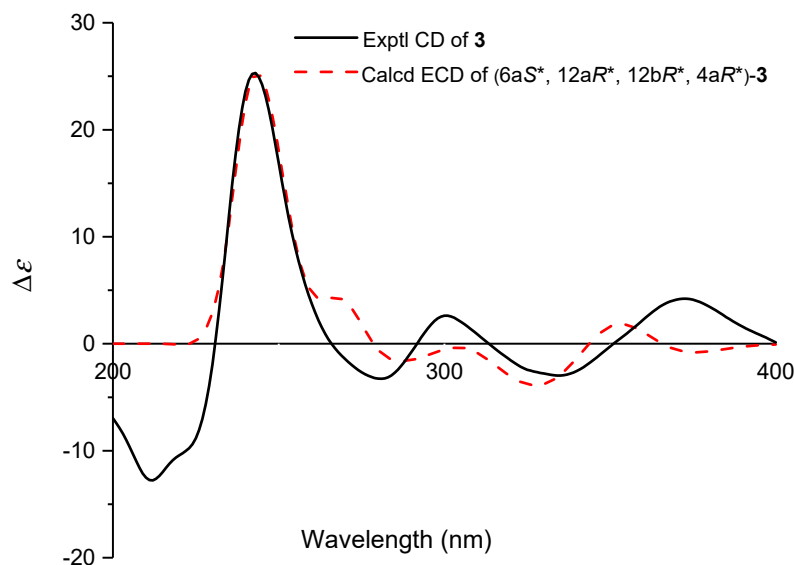


**Figure 5.** Calculated and experimental ECD spectra of **3**.

Compound **4** is a brown amorphous powder with molecular formula  $C_{19}H_{16}O_7$  deduced from HR-ESIMS, indicating 12 degrees of unsaturation. The  $^1H$  NMR spectrum of **4** displayed one methyl ( $\delta_H$  2.33, d,  $J = 1.2$  Hz), two methylenes ( $\delta_H$  1.98;  $\delta_H$  2.24, 2.14), five methines ( $\delta_H$  3.98, d,  $J = 1.3$  Hz;  $\delta_H$  3.14, s;  $\delta_H$  7.35, dd,  $J = 8.6, 1.0$  Hz;  $\delta_H$  7.76, dd,  $J = 8.3, 7.6$  Hz;  $\delta_H$  7.34, d,  $J = 7.5, 1.0$  Hz), a vinyl methine ( $\delta_H$  5.83, s), and three exchangeable protons ( $\delta_H$  5.59, s;  $\delta_H$  7.05, s;  $\delta_H$  11.72, s) (Table 1). The  $^{13}C$  NMR and HSQC spectrum showed that **4** contains one methyl ( $\delta_C$  26.3, q), two methylene ( $\delta_C$  26.8 and 32.6), six methines ( $\delta_C$  52.7, 85.1, 118.3, 123.7, 124.6, and 137.7), and ten quaternary carbons, including three non-protonated  $sp^3$  carbons ( $\delta_C$  78.0, 81.6 and 92.5), four non-protonated  $sp^2$  carbons ( $\delta_C$  114.9, 135.3, 161.1, and 162.4), and three carbonyls ( $\delta_C$  192.1, 195.6, and 201.6) (Table 2). The planar structure of **4** was then identified via a detailed analysis of 2D NMR (Figure 3). The A ring was determined by the HMBC correlations from H-2 ( $\delta_H$  5.83, s) to C-1 ( $\delta_C$  195.6), C-4 ( $\delta_C$  85.1), and C-12b ( $\delta_C$  52.7), from 13- $CH_3$  ( $\delta_H$  2.33, d) to C-2 ( $\delta_C$  124.6), C-3 ( $\delta_C$  162.4), C-4, and from H-4 ( $\delta_H$  3.98, d,  $J = 1.3$  Hz) to C-4a ( $\delta_C$  81.6) and C-12b. The  $^1H$ - $^1H$  COSY correlations from H-9 ( $\delta_H$  7.35, dd,  $J = 8.6, 1.0$  Hz) via H-10 ( $\delta_H$  7.76, dd,  $J = 8.3, 7.6$  Hz) through H-11 ( $\delta_H$  7.34, dd,  $J = 7.5, 1.0$  Hz) suggested the presence of the 1,2,3-trisubstituted benzene ring (ring D). HMBC correlation analyses from H-9 to C-7a ( $\delta_C$  114.9) and C-7 ( $\delta_C$  201.6), from H-10 to C-11a ( $\delta_C$  135.3) and C-8 ( $\delta_C$  161.1), and from H-11 to C-12 ( $\delta_C$  192.1) extend ring D to ring C. Further analysis of the HMBC correlations from H-5 ( $\delta_H$  1.98, m) to C-6a ( $\delta_C$  78.0) and C-12b and from H-6 ( $\delta_H$  2.14) to C-12a ( $\delta_C$  92.5) determined the presence of ring B, closing the angular skeleton of compound **4**. HMBC correlations from the active exchangeable protons 4a-OH ( $\delta_H$  5.59) to C-4a, C-4 and C-5 ( $\delta_C$  32.6), from 6a-OH ( $\delta_H$  7.05, s) to C-6a, C-7 and C-6, together with the fact that there are 12 degrees of unsaturation, suggests that another unsaturation should be the presence of an epoxide between C-12a and C-4 ( $\delta_C$  85.1). Thus, the planar structure of **4** was determined.

The stereo configuration of compound **4** was determined by NOESY spectral analysis and ECD calculations. The NOESY spectrum analysis revealed that H-12b ( $\delta_H$  3.14) correlates with 4a-OH and 6a-OH, indicating that H-12b, 4a-OH, and 6a-OH are in the same plane, resulting in only two possible structures: ( $4R^*, 4aR^*, 6aS^*, 12aS^*, 12bS^*$ )-**4** and ( $4S^*, 4aS^*, 6aR^*, 12aR^*, 12bR^*$ )-**4**. Finally, the absolute configuration of **4** was determined to be  $4S, 4aS, 6aR, 12aR$  based on the results of ECD calculations (Figure 6). Angucyclines carrying epoxide modifications on the skeletons were frequently discovered in nature [27], however, this is the first example of angucycline derivative with the epoxidation-bridged C-12a and C-4.

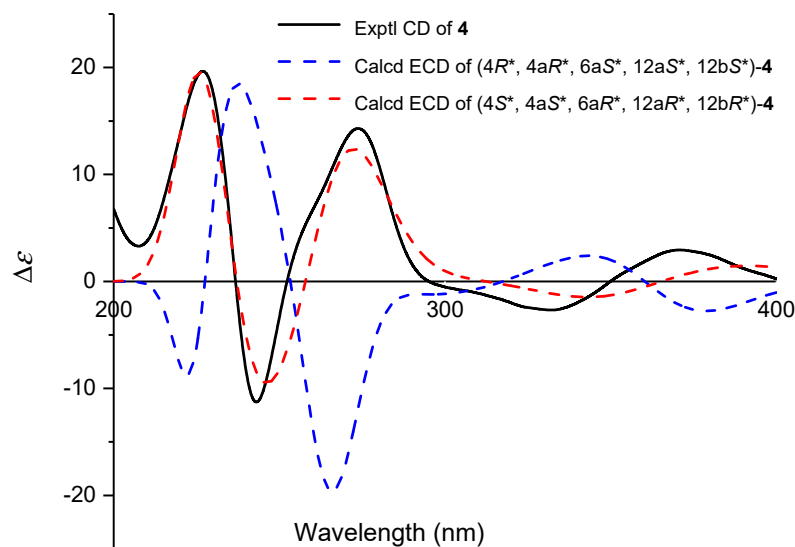


**Figure 6.** Calculated and experimental ECD spectra of 4.

Based on the comparison of NMR and MS data with those reported in the literature, the six known compounds isolated in this study were identified as WP 3688-2 (5) [28], gephyromycin (6) [29,30], SEK43 (7) [31], and SEK15 (8) [32].

All new angucyclines were evaluated for cytotoxicity against L-02, MDA-MB-231, K562, ASPC-1, and NCI-H446/EP cell lines *in vitro*. Adriamycin was used as the positive control. Compound 3 showed cytotoxicity toward five cancer cell lines and especially strongly inhibited K562 and NCI-H446/EP cell lines with IC<sub>50</sub> values of 11.72 and 8.92  $\mu$ M, respectively. It is worth mentioning that both compounds 3 and 4 possess an oxygen bridge and two hydroxyl groups in the structure; however, compound 4 did not display obvious cytotoxicity, which indicated that the oxidative modifications on rings A and B are very important for their mode of actions.

### 2.3. Plausible Biosynthetic Pathways for Compounds 1–8 Produced by the Mutant Strain

The plausible biogenetic pathway of compounds 1–8 was determined based on the bioinformatics analyses (Table S2) and literature surveys. First, the polyketide chain was generated by an iterative Claisen condensation reaction of a starting unit malonyl-CoA and nine extension unit malonyl-CoA under the action of the minimal PKS SpiA, SpiB and SpiC, and was subsequently folded by cyclase SpiE and SpiD to form UWM6 [33,34], a characteristic intermediate of angucyclines; however, if it is spontaneously folded, the by-products 7 and 8 will be produced. Thereafter, UWM6 can achieve the oxidation of C-12 catalyzed by monooxygenase SpiH2 [35] and subsequently undergo reduction at C-6, dehydration and enoyl reduction at C-5 and C-6, and oxidation at C-12b to produce 5, which could be converted into compounds 1 and 2 via a 6a, 12a-epoxide intermediate. The methanethiol residue of 2 was probably derived from methionine which was incorporated via methane thiol addition to the epoxide. In alternative routes, UWM6 may undergo multi-step catalysis including oxidation, dehydration and oxo-bridge generation to give 3, 4 and 6 in the presence of relevant endogenous enzymes of the heterologous host.

## 3. Materials and Methods

### 3.1. General Experimental Procedures

High-quality actinobacteria genomes were obtained using methods previously described in the literature [36,37]. Polymerase chain reaction (PCR) was performed using 2  $\times$  Phanta Flash Master Mix (P510, Vazyme, Nanjing, China). PCR analyses were conducted with a 2  $\times$  Hieff<sup>®</sup> PCR Master Mix (with dye, Yeasen, Shanghai, China). Shanghai Sangon DNA Technologies (Shanghai, China) offered custom oligonucleotide synthesis and fragment sequencing services.



NMR spectra were measured on an Agilent 500 MHz DD2 spectrometer with tetramethylsilane (TMS) as an internal standard. Optical rotations in MeOH were recorded on a JASCO-1020 digital polarimeter. A Thermo Scientific LTQ Orbitrap XL mass spectrometer (Thermo Fisher Scientific, Waltham, MA, USA) was used to collect HRESIMS data. UV-vis spectra were acquired on the UFLC system (Shimadzu, Tokyo, Japan). The JASCO J-715 spectropolarimeter was used to record the ECD spectra. A UFLC system (Shimadzu, Tokyo, Japan) with a C18 column (Shimadzu, 4.6 mm × 150 mm, 5 µm, 1 mL/min) coupled to an LCMS-2020 mass spectrometer (Shimadzu, Tokyo, Japan) was used to perform LC-MS analyses. Column chromatography (CC) was performed with SiliaSphere C18 (Octadecylsilyl, ODS) monomeric (SiliCycle Inc., Quebec, QC, Canada, 50 µm, 120 Å), and Sephadex LH-20 (GE Healthcare, Uppsala, Sweden). MPLC was performed using a C18 column (Welch Materials Inc., Ultimate® XB-C18, 21.2 mm × 250 mm, 5 µm, 10 mL/min).

Prediction and analysis of gene clusters using the online tool antiSMASH. DNA and protein sequence homology analysis using the online tool NCBI.

### 3.2. Materials and Culture Conditions

*Streptomyces* sp. HDN155000 was obtained from a marine sediment sample collected from the South China Sea at coordinates 125°28.550' E and 29°1.618' N. The strain was identified via genome sequencing and submitted to GenBank (accession number MN822699). *S. albus* J1074 was grown for 6 days at 28 °C on MS plates with 2% mannitol, 2% soya bean flour, and 1.5% agar. For genome extraction, the strain was inoculated into 250 mL Erlenmeyer flasks containing 50 mL of TSB liquid medium (1.7% tryptone, 0.3% peptone, 0.25% glucose, 0.25% KH<sub>2</sub>PO<sub>4</sub>, and 0.3% NaCl) for 4 days.

*Escherichia coli* strains DH10B as the general host for cloning and *E. coli* ET12567/pUZ8002 as the donor in intergeneric conjugation were cultured on Luria–Bertani plates or liquid medium (1% tryptone, 0.5% yeast extract, and 1% NaCl) at 37 °C.

### 3.3. *S. albus* J1074 Intergeneric Conjugation

The intergeneric conjugation between *E. coli* and *S. albus* J1074 was performed as previously described with some modifications [38]. The culture of the donor *E. coli* ET12567/pUZ8002 containing the heterologous vector p15A::spi was incubated with appropriate antibiotics LB liquid culture medium (containing 50 mg/L kanamycin, 15 mg/L chloramphenicol, and 50 mg/L apramycin,) until the optical density at 600 nm (OD<sub>600</sub>) of 0.6–0.8. Bacteriophages were collected at 9000 rpm, rinsed three times with 1 mL 2 × YT medium [39] to remove antibiotics, and then resuspended in 0.2 mL of 2 × YT (containing 10 mM MgCl<sub>2</sub>) as the donor cells. *S. albus* J1074 spores were washed three times and suspended in 2 × YT broth at a concentration of 10<sup>9</sup> per mL. Subsequently, spores obtained in the previous step were heated at 50 °C for 10 min to serve as recipients. Donor and recipient cells were mixed evenly on MS plates (containing 30 mM MgCl<sub>2</sub> and 30 mM CaCl<sub>2</sub>), and cultivated for 18 h at 30 °C. After incubation, plates were covered with 1 mL of water with apramycin (50 µg/mL) and nalidixic acid (50 µg/mL) and then kept at 30 °C for 4–6 days until exconjugants appeared. The conjugation frequency reached 7.8 × 10<sup>-5</sup>.

### 3.4. Fermentation and LC/LC-MS Analysis

Heterologous expression strains and negative control strains were cultured for 7 days at 28 °C in 500 mL Erlenmeyer flasks with 100 mL of M1 medium (2 g/L peptone, 4 g/L yeast extract, 10 g/L starch), after which the culture products were collected and extracted three times with ethyl acetate. The organic phase was evaporated, and the residue was re-dissolved in 150 µL MeOH, which was analyzed using HPLC (C18 column, Shimadzu, 4.6 mm × 150 mm, 5 µm, 1 mL/min), revealing a considerable change in metabolite synthesis in the heterologous expression strain J1074::spi (Figure 1).

For the isolation of secondary metabolites, we scaled up cultures with the 500 mL Erlenmeyer flask (total 20 L) according to the conditions used for small-scale analyses. The

fermentation supernatant was extracted with ethyl acetate three times and then evaporated to dryness, obtaining a total of 11.3 g of crude product.

### 3.5. Extraction, Isolation, and Purification

The crude extract was eluted using a step gradient of MeOH-H<sub>2</sub>O using metabolite detection on a C18 column, yielding seven subfractions (Fr.1-Fr.7, 30% to 100%). Fr.2 was purified by semi-preparative HPLC (33:67 MeOH-H<sub>2</sub>O, 3 mL/min) to generate compounds **1** (7.1 mg, *t<sub>R</sub>* = 15.1 min) and **6** (3.1 mg, *t<sub>R</sub>* = 16.7 min). Fr.3 was purified by a semi-preparative C18 HPLC column (47:53 MeOH-H<sub>2</sub>O), producing compound **3** (6.4 mg, *t<sub>R</sub>* = 14.7 min). Fr.4 was separated using preparative C18 HPLC column (58:42 MeOH-H<sub>2</sub>O) to yield two sub-fractions (Fr.4.1 and Fr.4.2). Then, Fr.4.1 and Fr.4.2 were purified by semi-preparative HPLC (53:47, 60:40, MeOH-H<sub>2</sub>O, 3 mL/min) to provide compounds **4** (4.7 mg, *t<sub>R</sub>* = 18.1 min), **5** (3.4 mg, *t<sub>R</sub>* = 20.7 min), **7** (3.8 mg, *t<sub>R</sub>* = 16.9 min), and **8** (3.0 mg, *t<sub>R</sub>* = 19.4 min), respectively. Fr.5 was applied to a Sephadex LH-20 column and eluted with methanol, obtaining compound **2** (5.6 mg).

Angumycinone Z (**1**): pale brown powder,  $[\alpha]_D^{25} + 19.5$  (*c* 0.03, CH<sub>3</sub>OH); UV (DAD)  $\lambda_{\max}$  208 nm, 250 nm, 327 nm, 386 nm; CD (MeOH)  $\lambda_{\max}$  ( $\Delta\epsilon$ ) 210 (−19.06), 243 (+33.91), 283 (−4.88), 302 (+3.13), 336 (−3.39), 376 (+5.21); <sup>1</sup>H and <sup>13</sup>C NMR data, see Tables 1 and 2; negative ion HRESIMS *m/z* 373.0916 [M − H]<sup>−</sup> (calcd. for C<sub>19</sub>H<sub>17</sub>O<sub>7</sub><sup>−</sup>, 373.0928).

WS009 Z (**2**): even brown amorphous powder,  $[\alpha]_D^{25} + 55.8$  (*c* 0.03, CH<sub>3</sub>OH); UV (DAD)  $\lambda_{\max}$  249, 302, 352; <sup>1</sup>H and <sup>13</sup>C NMR data, see Tables 1 and 2; positive ion HRESIMS *m/z* 405.0996 [M + H]<sup>+</sup> (calcd. for C<sub>20</sub>H<sub>21</sub>O<sub>7</sub>S<sup>+</sup>, 405.1003).

Angumycinone X (**3**): yellowish, solid powder,  $[\alpha]_D^{25} + 79.1$  (*c* 0.03, CH<sub>3</sub>OH); UV (DAD)  $\lambda_{\max}$  206, 238, 309, 364; CD (MeOH)  $\lambda_{\max}$  ( $\Delta\epsilon$ ) 211 (−12.77), 242 (+25.31), 281 (−3.28), 300 (+2.63), 334 (−2.96), 372 (+4.21); <sup>1</sup>H and <sup>13</sup>C NMR data, see Tables 1 and 2; negative ion HRESIMS *m/z* 355.0821 [M − H]<sup>−</sup> (calcd. for C<sub>19</sub>H<sub>15</sub>O<sub>7</sub><sup>−</sup>, 355.0823).

Angumycinone T (**4**): brown amorphous powder,  $[\alpha]_D^{25} + 31.0$  (*c* 0.03, CH<sub>3</sub>OH); UV (DAD)  $\lambda_{\max}$  206, 236, 298, 350; CD (MeOH)  $\lambda_{\max}$  ( $\Delta\epsilon$ ) 207 (+3.30), 227 (+19.67), 243 (−11.30), 274 (+14.31), 332 (−2.67), 370 (+2.94); <sup>1</sup>H and <sup>13</sup>C NMR data, see Tables 1 and 2; negative ion HRESIMS *m/z* 355.0815 [M − H]<sup>−</sup> (calcd. for C<sub>19</sub>H<sub>15</sub>O<sub>7</sub><sup>−</sup>, 355.0823).

### 3.6. NMR and ECD Calculations

Conformation searches based on molecular mechanics with MMFF force fields were performed for stereoisomers to obtain stable conformers. The Gaussian 16 programme package [40] used the density functional theory (DFT) approach at the B3LYP/6-31G(d) level to optimize all conformers. Gauge Independent Atomic Orbital (GIAO) calculations of their <sup>1</sup>H and <sup>13</sup>C NMR chemical shifts were performed utilizing density functional theory (DFT) at the mPW1PW91/6-311+G(d,p) level with the PCM model in DMSO [41]. The calculated NMR data of these conformers were averaged using the Boltzmann distribution theory and their respective Gibbs free energy. The <sup>1</sup>H and <sup>13</sup>C NMR chemical shifts for TMS were computed using the same methodology and served as a reference. Following calculation, the experimental and calculated data were compared using linear correlation coefficients (R<sup>2</sup>) and the improved probability DP4+ technique [42].

All stable conformers were further optimized at the B3LYP/6-31G(d)-GD3BJ level with the Gaussian 16 programme package. The ECD was computed using time-dependent density functional theory (TDDFT) at a B3LYP/6-311+G(d,p) level with the IEFPCM model. The calculated ECD curves were all generated using the SpecDis 1.71 computer package and the calculated ECD data of all conformers were Boltzmann averaged using Gibbs free energy [43].

### 3.7. Cytotoxicity Assay

The cytotoxic assay involved five human cancer cell lines: K562 (using the MTT method), ASPC-1, NCI-H446/EP, MDA-MB-231, and L-02 (using the SRB method). Adriamycin (ADM) was employed as a positive control. The detailed procedures for biological

testing were conducted as previously stated [20,44]. The cancer cell lines are purchased from the National Collection of Authenticated Cell Cultures of China (Shanghai).

#### 4. Conclusions

Secondary metabolites from actinobacteria have long been a valuable source of natural medicines [45]. However, the success rate for identifying actinobacteria-derived novel compounds is limited by gene cluster silencing or low expression under laboratory conditions, especially for micro-organisms from special habitats such as marine actinobacteria. In this study, the type II PKS gene cluster *spi* derived from *Streptomyces* sp. HDN155000 was successfully heterologously expressed in *S. albus* J1074, and a total of eight compounds were obtained through further fermentation, isolation, and purification. Based on the literature and our previous study, we proposed a plausible biosynthetic pathway leading to those new compounds [4,34]. Generally, compounds 3–6 were directly produced from UWM6 by a multi-step enzymatic reaction involving oxidation, dehydration, enoyl reduction, etc. Compounds 1 and 2 were derived from compound 5 via dehydrogenation, hydrolysis, methane thiol addition, and other processes. Angucyclines are a chemical family that has been extensively explored in actinobacteria since the first structure was described in 1965 in *Streptomyces rimosus* [2]. More than 400 cases have been recorded, with a range of skeleton modifications; however, compound 4 is the first example of oxidized angucyclines with an oxo-bridge between C-12a and C-4 [3]. Compound 3 showed cytotoxic to the K562 and NCI-H446/EP cell lines, providing an alternative lead compound for the study of human chronic myeloid leukemia and lung cancer. The above data enrich our understanding of the type II PKS pathways and related aromatic products, and also indicate heterologous expression as a promising strategy for maximizing the metabolic capability of *Streptomyces*.

**Supplementary Materials:** The following supporting information can be downloaded at: <https://www.mdpi.com/article/10.3390/md22110480/s1>, Figure S1: Restriction to validate heterologous expression plasmid p15A-*spi* and PCR analysis for confirming the heterologous strain J1074::*spi*; Figure S2: Comparative analysis of metabolites from two heterologous hosts, *S. albus* J1074 and *S. coelicolor* A3; Figure S3: <sup>13</sup>C NMR calculation results of four possible isomers of 3; Figures S4–S10: NMR and HRESIMS spectra of compound 1; Figures S11–S16: NMR and HRESIMS spectra of compound 2; Figures S17–S22: NMR and HRESIMS spectra of compound 3; Figures S23–S29: NMR and HRESIMS spectra of compound 4; Table S1: The primers used in this study; Table S2: Deduced function of 25 genes in *spi*; Table S3–S6: Calculated <sup>13</sup>C NMR results for 3a, 3b, 3c, 3d; Table S7: DP4+ analysis results of 3a (Isomer 1), 3b (Isomer 2), 3c (Isomer 3) and 3d (Isomer 4).

**Author Contributions:** The contributions of the respective authors are as follows: X.Z. drafted the work and performed isolation and structural elucidation of the extract. X.Z. and F.Z. performed the NMR and ECD Calculations of the compounds. Biological evaluations were performed by C.L., J.L., X.X., T.Z., Q.C. and D.L. checked the procedures of this work. G.Z. designed the project and contributed to the critical reading of the manuscript. All authors have read and agreed to the published version of the manuscript.

**Funding:** This research was funded by the National Natural Science Foundation of China (81991522, 32370061), Qingdao Marine Science and Technology Center (2022QNLM030003-1, 2022QNLM030003-2), NSFC-Shandong Joint Fund (U1906212), Hainan Provincial Joint Project of Sanya Yazhou Bay Science and Technology City (2021CXLH0012), Taishan Scholar Youth Expert Program in Shandong Province (tsqn 202103153), Major Basic Research Programs of Natural Science Foundation of Shandong Province (ZR2021ZD28).

**Institutional Review Board Statement:** Not applicable.

**Data Availability Statement:** The data given in this research are available in this article and the Supplementary Materials.

**Acknowledgments:** We thank Bin Wang (Institute of Microbiology, Chinese Academy of Sciences) for providing the heterologous expression strain.

**Conflicts of Interest:** The authors declare no conflicts of interest.

## References

1. Rohr, J.; Thiericke, R. Angucycline group antibiotics. *Nat. Prod. Rep.* **1992**, *9*, 103–137. [[CrossRef](#)] [[PubMed](#)]
2. Zhang, J.; Duan, Y.; Zhu, X.; Yan, X. Novel angucycline/angucyclinone family of natural products discovered between 2010 and 2020. *Sheng Wu Gong Cheng Xue Bao* **2021**, *37*, 2147–2165. [[PubMed](#)]
3. Hibi, G.; Shiraishi, T.; Umemura, T.; Nemoto, K.; Ogura, Y.; Nishiyama, M.; Kuzuyama, T. Discovery of type II polyketide synthase-like enzymes for the biosynthesis of cispentacin. *Nat. Commun.* **2023**, *14*, 8065. [[CrossRef](#)] [[PubMed](#)]
4. Metsä-Ketelä, M.; Palmu, K.; Kunnari, T.; Ylihonko, K.; Mäntsälä, P. Engineering anthracycline biosynthesis toward angucyclines. *Antimicrob. Agents Chemother.* **2003**, *47*, 1291–1296. [[CrossRef](#)]
5. Watve, M.G.; Tickoo, R.; Jog, M.M.; Bhole, B.D. How many antibiotics are produced by the genus *Streptomyces*? *Arch. Microbiol.* **2001**, *176*, 386–390. [[CrossRef](#)]
6. van Bergeijk, D.A.; Terlouw, B.R.; Medema, M.H.; van Wezel, G.P. Ecology and genomics of Actinobacteria: New concepts for natural product discovery. *Nat. Rev. Microbiol.* **2020**, *18*, 546–558. [[CrossRef](#)]
7. Liu, Y.; Yue, S.J.; Wang, W.; Hu, H.B.; Zhang, X.H. Elucidation of the biosynthesis of griseoluteic acid in *Streptomyces griseoluteus* P510. *J. Nat. Prod.* **2024**, *87*, 1540–1547. [[CrossRef](#)]
8. Nett, M.; Ikeda, H.; Moore, B.S. Genomic basis for natural product biosynthetic diversity in the actinomycetes. *Nat. Prod. Rep.* **2009**, *26*, 1362–1384. [[CrossRef](#)]
9. Lopatkin, A.J.; Bening, S.C.; Manson, A.L.; Stokes, J.M.; Kohanski, M.A.; Badran, A.H.; Earl, A.M.; Cheney, N.J.; Yang, J.H.; Collins, J.J. Clinically relevant mutations in core metabolic genes confer antibiotic resistance. *Science* **2021**, *371*, eaba0862. [[CrossRef](#)]
10. Platon, V.M.; Dragoi, B.; Marin, L. Erythromycin formulations-A journey to advanced drug delivery. *Pharmaceutics* **2022**, *14*, 2180. [[CrossRef](#)]
11. Chopra, I.; Roberts, M. Tetracycline antibiotics: Mode of action, applications, molecular biology, and epidemiology of bacterial resistance. *Microbiol. Mol. Biol. Rev. MMBR* **2001**, *65*, 232–260. [[CrossRef](#)] [[PubMed](#)]
12. Katz, M.; Hover, B.M.; Brady, S.F. Culture-independent discovery of natural products from soil metagenomes. *J. Ind. Microbiol. Biotechnol.* **2016**, *43*, 129–141. [[CrossRef](#)] [[PubMed](#)]
13. Zhang, J.J.; Tang, X.; Moore, B.S. Genetic platforms for heterologous expression of microbial natural products. *Nat. Prod. Rep.* **2019**, *36*, 1313–1332. [[CrossRef](#)]
14. Liu, Z.; Sun, W.; Hu, Z.; Wang, W.; Zhang, H. Marine *Streptomyces*-derived novel alkaloids discovered in the past decade. *Mar. Drugs* **2024**, *22*, 51. [[CrossRef](#)] [[PubMed](#)]
15. Yang, Z.; He, J.; Wei, X.; Ju, J.; Ma, J. Exploration and genome mining of natural products from marine *Streptomyces*. *Appl. Microbiol. Biotechnol.* **2020**, *104*, 67–76. [[CrossRef](#)]
16. Poli, A.; Finore, I.; Romano, I.; Gioiello, A.; Lama, L.; Nicolaus, B. Microbial diversity in extreme marine habitats and their biomolecules. *Microorganisms* **2017**, *5*, 25. [[CrossRef](#)]
17. Rodríguez Estévez, M.; Myronovskyi, M.; Gummerlich, N.; Nadmid, S.; Luzhetskyy, A. Heterologous expression of the nybomycin gene cluster from the marine strain *Streptomyces albus* subsp. chlorinus NRRL B-24108. *Mar. Drugs* **2018**, *16*, 435. [[CrossRef](#)]
18. Liu, S.H.; Wang, W.; Wang, K.B.; Zhang, B.; Li, W.; Shi, J.; Jiao, R.H.; Tan, R.X.; Ge, H.M. Heterologous expression of a cryptic giant Type I PKS gene cluster leads to the production of ansaseomycin. *Org. Lett.* **2019**, *21*, 3785–3788. [[CrossRef](#)]
19. Klumbys, E.; Xu, W.; Koduru, L.; Heng, E.; Wei, Y.; Wong, F.T.; Zhao, H.; Ang, E.L. Discovery, characterization, and engineering of an advantageous *Streptomyces* host for heterologous expression of natural product biosynthetic gene clusters. *Microb. Cell Fact.* **2024**, *23*, 149. [[CrossRef](#)]
20. Xu, X.; Chang, Y.; Chen, Y.; Zhou, L.; Zhang, F.; Ma, C.; Che, Q.; Zhu, T.; Pfeifer, B.A.; Zhang, G.; et al. Biosynthesis of Atypical Angucyclines Unveils New Ring Rearrangement Reactions Catalyzed by Flavoprotein Monooxygenases. *Org. Lett.* **2024**, *26*, 7489–7494. [[CrossRef](#)]
21. Hoz, J.F.; Méndez, C.; Salas, J.A.; Olano, C. Novel Bioactive Paulomycin Derivatives Produced by *Streptomyces albus* J1074. *Molecules* **2017**, *22*, 1758. [[CrossRef](#)]
22. Yuan, H.; Zheng, Y.; Yan, X.; Wang, H.; Zhang, Y.; Ma, J.; Fu, J. Direct cloning of a herpesvirus genome for rapid generation of infectious BAC clones. *J. Adv. Res.* **2023**, *43*, 97–107. [[CrossRef](#)] [[PubMed](#)]
23. Fu, S.; An, Z.; Wu, L.; Xiang, Z.; Deng, Z.; Liu, R.; Liu, T. Evaluation and optimization of analytical procedure and sample preparation for polar *Streptomyces albus* J1074 metabolome profiling. *Synth. Syst. Biotechnol.* **2022**, *7*, 949–957. [[CrossRef](#)]
24. Cao, M.; Zheng, C.; Yang, D.; Kalkreuter, E.; Adhikari, A.; Liu, Y.C.; Rateb, M.E.; Shen, B. Cryptic Sulfur incorporation in thioangucycline biosynthesis. *Angew. Chem. Int. Ed. Engl.* **2021**, *60*, 7140–7147. [[CrossRef](#)]
25. Kharel, M.K.; Pahari, P.; Shepherd, M.D.; Tibrewal, N.; Nybo, S.E.; Shaaban, K.A.; Rohr, J. Angucyclines: Biosynthesis, mode-of-action, new natural products, and synthesis. *Nat. Prod. Rep.* **2012**, *29*, 264–325. [[CrossRef](#)]
26. Su, H.; Shao, H.; Zhang, K.; Li, G. Antibacterial metabolites from the Actinomycete *Streptomyces* sp. P294. *J. Microbiol.* **2016**, *54*, 131–135. [[CrossRef](#)] [[PubMed](#)]
27. Jackson, D.R.; Yu, X.; Wang, G.; Patel, A.B.; Calveras, J.; Barajas, J.F.; Sasaki, E.; Metsä-Ketelä, M.; Liu, H.W.; Rohr, J.; et al. Insights into complex oxidation during BE-7585A biosynthesis: Structural determination and analysis of the polyketide monooxygenase BexE. *ACS Chem. Biol.* **2016**, *11*, 1137–1147. [[CrossRef](#)] [[PubMed](#)]
28. Gould, S.J.; Cheng, X.C. New benz[a]anthraquinone secondary metabolites from *Streptomyces phaeochromogenes*. *J. Org. Chem.* **1994**, *59*, 400–405. [[CrossRef](#)]

29. Gao, H.M.; Xie, P.F.; Zhang, X.L.; Yang, Q. Isolation, phylogenetic and gephyromycin metabolites characterization of new exopolysaccharides-bearing antarctic actinobacterium from feces of emperor penguin. *Mar. Drugs* **2021**, *19*, 458. [[CrossRef](#)]
30. Bringmann, G.; Lang, G.; Maksimenka, K.; Hamm, A.; Gulder, T.A.; Dieter, A.; Bull, A.T.; Stach, J.E.; Kocher, N.; Müller, W.E. Fiedler HP. Gephyromycin, the first bridged angucyclinone, from *Streptomyces griseus* strain NTK 14. *Phytochemistry* **2005**, *66*, 1366–1373. [[CrossRef](#)]
31. Gao, Y.; Zhao, Y.; Zhou, J.; Yang, M.; Lin, L.; Wang, W.; Tao, M.; Deng, Z.; Jiang, M. Unexpected role of a short-chain dehydrogenase/reductase family protein in Type II polyketide biosynthesis. *Angew. Chem. Int. Ed. Engl.* **2022**, *61*, e202110445. [[CrossRef](#)]
32. Ridley, C.P.; Khosla, C. Synthesis and biological activity of novel pyranopyrones derived from engineered aromatic polyketides. *ACS Chem. Biol.* **2007**, *2*, 104–108. [[CrossRef](#)]
33. Xu, D.; Metz, J.; Harmody, D.; Peterson, T.; Winder, P.; Guzmán, E.A.; Russo, R.; McCarthy, P.J.; Wright, A.E.; Wang, G. Brominated and sulfur-containing angucyclines derived from a single pathway: Identification of nocardiosistins D-F. *Org. Lett.* **2022**, *24*, 7900–7904. [[CrossRef](#)]
34. Chen, Y.H.; Wang, C.C.; Greenwell, L.; Rix, U.; Hoffmeister, D.; Vining, L.C.; Rohr, J.; Yang, K.Q. Functional analyses of oxygenases in jadomycin biosynthesis and identification of JadH as a bifunctional oxygenase/dehydrase. *J. Biol. Chem.* **2005**, *280*, 22508–22514. [[CrossRef](#)] [[PubMed](#)]
35. Yang, C.; Zhang, L.; Zhang, W.; Huang, C.; Zhu, Y.; Jiang, X.; Liu, W.; Zhao, M.; De, B.C.; Zhang, C. Biochemical and structural insights of multifunctional flavin-dependent monooxygenase FlsO1-catalyzed unexpected xanthone formation. *Nat. Commun.* **2022**, *13*, 5386. [[CrossRef](#)] [[PubMed](#)]
36. Monciardini, P.; Iorio, M.; Maffioli, S.; Sosio, M.; Donadio, S. Discovering new bioactive molecules from microbial sources. *Microb. Biotechnol.* **2014**, *7*, 209–220. [[CrossRef](#)] [[PubMed](#)]
37. Enghiad, B.; Huang, C.; Guo, F.; Jiang, G.; Wang, B.; Tabatabaei, S.K.; Martin, T.A.; Zhao, H. Cas12a-assisted precise targeted cloning using in vivo Cre-lox recombination. *Nat. Commun.* **2021**, *12*, 1171. [[CrossRef](#)] [[PubMed](#)]
38. Hou, Y.H.; Li, F.C.; Wang, S.J.; Qin, S.; Wang, Q.F. Intergeneric conjugation in holomycin-producing marine *Streptomyces* sp. strain M095. *Microbiol. Res.* **2008**, *163*, 96–104. [[CrossRef](#)]
39. Du, L.; Liu, R.H.; Ying, L.; Zhao, G.R. An efficient intergeneric conjugation of DNA from *Escherichia coli* to mycelia of the lincomycin-producer *Streptomyces lincolnensis*. *Int. J. Mol. Sci.* **2012**, *13*, 4797–4806. [[CrossRef](#)]
40. Frisch, M.J.; Trucks, G.W.; Schlegel, H.B.; Scuseria, G.E.; Robb, M.A.; Cheeseman, J.R.; Scalmani, G.; Barone, V.; Petersson, G.A.; Nakatsuji, H.; et al. *Gaussian 16, Revision B.01*; Gaussian, Inc.: Wallingford, CT, USA, 2016.
41. Xu, X.; Zhang, F.; Zhou, L.; Chang, Y.; Che, Q.; Zhu, T.; Li, D.; Zhang, G. Overexpression of global regulator SCrp leads to the discovery of new angucyclines in *Streptomyces* sp. XS-16. *Mar. Drugs* **2023**, *21*, 240. [[CrossRef](#)]
42. Marcarino, M.O.; Cicetti, S.; Zanardi, M.M.; Sarotti, A.M. A critical review on the use of DP4+ in the structural elucidation of natural products: The good, the bad and the ugly. A practical guide. *Nat. Prod. Rep.* **2022**, *39*, 58–76. [[CrossRef](#)] [[PubMed](#)]
43. Bruhn, T.; Schaumlöffel, A.; Hemberger, Y.; Bringmann, G. SpecDis: Quantifying the comparison of calculated and experimental electronic circular dichroism spectra. *Chirality* **2013**, *25*, 243–249. [[CrossRef](#)] [[PubMed](#)]
44. Zhang, F.; Ma, C.; Che, Q.; Zhu, T.; Zhang, G.; Li, D. Extending the structural diversity of labdane diterpenoids from marine-derived fungus *Talaromyces* sp. HDN151403 using heterologous expression. *Mar. Drugs* **2023**, *21*, 628. [[CrossRef](#)] [[PubMed](#)]
45. Lewis, K. The science of antibiotic discovery. *Cell* **2020**, *181*, 29–45. [[CrossRef](#)]

**Disclaimer/Publisher’s Note:** The statements, opinions and data contained in all publications are solely those of the individual author(s) and contributor(s) and not of MDPI and/or the editor(s). MDPI and/or the editor(s) disclaim responsibility for any injury to people or property resulting from any ideas, methods, instructions or products referred to in the content.